Drug Deliv. and Transl. Res. (2015) 5:438–450
DOI 10.1007/s13346-015-0245-z

RESEARCH ARTICLE

Fabrication of photomasks consisting microlenses for the production of polymeric microneedle array

Himanshu Kathuria[1] · **Michelle H. M. Fong**[1] · **Lifeng Kang**[1]

Published online: 25 July 2015

Abstract A photomask consisting plano-convex microlenses for the production of polymeric microneedles was fabricated from a microinjection array. The microinjection array was first fabricated using photolithographical approach and subsequently assembled onto a polydimethylsiloxane (PDMS) stamp. Poly (ethylene glycol) diacrylate (PEGDA) solution was loaded into the microinjection stamp. The microinjection stamp was then applied onto a coverslip to dispense the polymer solution, producing liquid microdroplets. They were then irradiated to form plano-convex microlenses. These microlenses were evaluated for their geometric properties and were fabricated into photomasks. The photomask consisting microlenses was used to fabricate polymeric microneedles that were evaluated and tested for skin penetration efficiency.

Keywords Microneedle · Microinjection · Microlens · Hydrogel · Photolithography

Introduction

Transdermal drug delivery offers an appealing alternative for administration of both oral and hypodermic dosage forms of biotechnology-based drugs [1]. It has many advantages including improved patient compliance, avoidance of first pass effect, and non-invasiveness [2, 3]. However, drug permeation through the skin has been shown to be limited by the stratum corneum (SC) acting as a physical barrier to exogenous substances [4]. Various chemical, physical, and mechanical strategies, such as chemical penetration enhancers, pressure waves, and iontophoresis, were used to overcome this barrier [5].

One of the promising approaches to overcome the barrier is the use of microneedles, which penetrate the SC, creating micron-sized channels into the underlying tissues for direct delivery of the therapeutics [6]. These needles are small enough to avoid fear and pain, and allow self-administration [7]. Recently, there has been extensive interest in microneedles and its fabrication [8]. Conventional microfabrication techniques involve the use of etching, laser cutting, metal electroplating, and micromolding, alone or in combination, to generate microstructures using varying materials such as polymers and metals [9–11].

Photolithography in combination with photomask consisting microlenses has also been used to fabricate the microneedle arrays. Microlenses are widely seen in biodetection systems [12, 13], biomedical imaging [14], and optical communications [15], to collect light, change the focal length, and steer light beams [16]. Thus, many sophisticated microlens fabrication methods have been reported, such as reflowing [17, 18], etching [19], molding [20], and stamping [21]. With its ability to alter the pathway of UV light, a method has been developed to fabricate microneedles by using photolithography in combination with photomask consisting concave microlenses [22].

Recently, a new method was developed in our lab to simplify sharp microneedle fabrication by using photomasks integrated with isotropically etched convex microlenses [23]. However, the lens surfaces were found to be flat and not convex, due largely to manner in which the chemicals etched into

Himanshu Kathuria and Michelle H. M. Fong contributed equally to this work.

✉ Lifeng Kang
lkang@nus.edu.sg

[1] Department of Pharmacy, National University of Singapore, 18 Science Drive 4, Singapore 117543, Singapore

the wafer. These lenses had unpredictable effects leading to formation of irregular microneedle tips in some cases. This has motivated us to find an alternative method to fabricate the photomask consisting microlenses with convex surfaces.

In this study, a microinjection array was used to dispense microdroplets of prepolymer solution containing poly (ethylene glycol) diacrylate (PEGDA), a photocurable macromer [24]. The microdroplet array was then cured by UV light to form plano-convex microlenses. These microlenses were found to possess appropriate geometric properties, key to optically modifying UV light path to fabricate microneedles that are shorter and sharper.

Materials and methods

Materials

PEGDA (Mn=250), PEGDA (Mn=575), PEGDA (Mn=700), 2-hydroxy-2-methyl-propiophenone (HMP) and 3-(trimethoxysilyl) propyl methacrylate (TMSPMA) were purchased from Sigma-Aldrich (St. Louis, MO). Silicone elastomer base solution and curing agent Sylgard 184 were purchased from Dow Corning Corporation (Midland, USA). All materials were reagent grade and were used as received.

Fabrication of microinjection array

Coating of glass slides and coverslips

Glass slides (Corning, USA, 1.06 mm thickness, 75×50 mm) and glass coverslips (Menzel Glaser, Germany, 190 μm thickness, 22×22 mm) were rinsed with 70 % ethanol and air-dried. They were immersed in 0.4 % TMSPMA solution for coating overnight. The glass slides and coverslips were then washed with water and baked for 2 h at 70 °C. Silanol groups on the glass will attach onto the TMSPMA molecules [25].

Fabrication of backing layer

A setup was made on a TMSPMA-coated glass slide as seen in Fig. 1. A cavity was created using coverslips as shown in Fig. 1b. The number of coverslips used determines the height of the cavity (spacer thickness). A photomask is a plastic film inked specifically to a pattern. The backing layer photomask had inked circles with a center-to-center spacing of 1500 μm. The microinjection array photomask had inked circles, with a center-to-center spacing of 1500 μm, that were surrounded by a circle of larger diameter. Figure 1 and Table 2 show dimensions of the two photomasks, for the backing layer and microinjection array. These were designed separately using AutoCAD 2014 and printed using high-resolution (8000 dpi) printer on the plastic film of 7 mil (Infinite Graphics, Singapore). During all steps of fabrication, ink/emulsion side of the photomask was facing the UV light source. Assembly of two photomask (for backing and microinjection array) was done manually utilizing the Nikon SMZ25 stereomicroscope (Nikon, Japan) to confirm that alignment was done appropriately. The inked regions blocked UV access while surrounding transparent regions allowed UV light to pass through to photopolymerize the polymer solution. Both photomasks had to be aligned such that all inked circles of both the backing layer photomask and the microinjection photomask overlapped (see Fig. 1), for microinjections to form onto the backing layer directly. To facilitate the alignment of the photomasks in later steps, prealignment of both photomask was necessary as shown in Fig. 1c, d. The aligned photomasks were laid opened, flat down, and the backing layer photomask was secured onto the front side of the setup with tape on all three sides. The microinjection photomask was folded down and secured with tape on one side.

On the back side of the setup, an uncoated coverslip was placed over the cavity and filled with PEGDA (Mn=250) containing 0.5 % *w*/*w* HMP (referred to as prepolymer solution). The setup was then flipped over and irradiated with UV of desired intensity and time of exposure, at a distance of 10 cm using a UV curing station with a UV filter range of 320–500 nm (OmniCure® S2000, EXFO Photonics Solutions Inc., Canada). The UV intensity was measured with OmniCure® R2000 radiometer. A collimating adaptor (EXFO 810–00043) was used with the UV light probe. Following polymerization, the coverslip was removed and the backing layer formed on the setup was rinsed with running water and dried using compressed air (Fig. 2a). This prevented undesired polymerization of the backing layer, as a result of any residue unpolymerized prepolymer solution present, during the fabrication of the microinjection array.

Fabrication of microinjections

The microinjection photomask was folded over the backing layer photomask with proper alignment, assisted by the prealignment step (Fig. 1d). Later on the back side of the setup now containing the backing layer, an uncoated coverslip was placed over the cavity, 5-coverlips in thickness, and filled with the prepolymer solution. The setup was flipped over and irradiated at a UV intensity of 3.82 W/cm^2 for a desired time of exposure, at a distance of 10 cm from the UV source. Following polymerization, the microinjection array formed was carefully removed, rinsed with running water, and dried using compressed air (Fig. 2b). The array was then irradiated with 7.95 W/cm^2 UV intensity for 2 s at a distance of 10 cm,

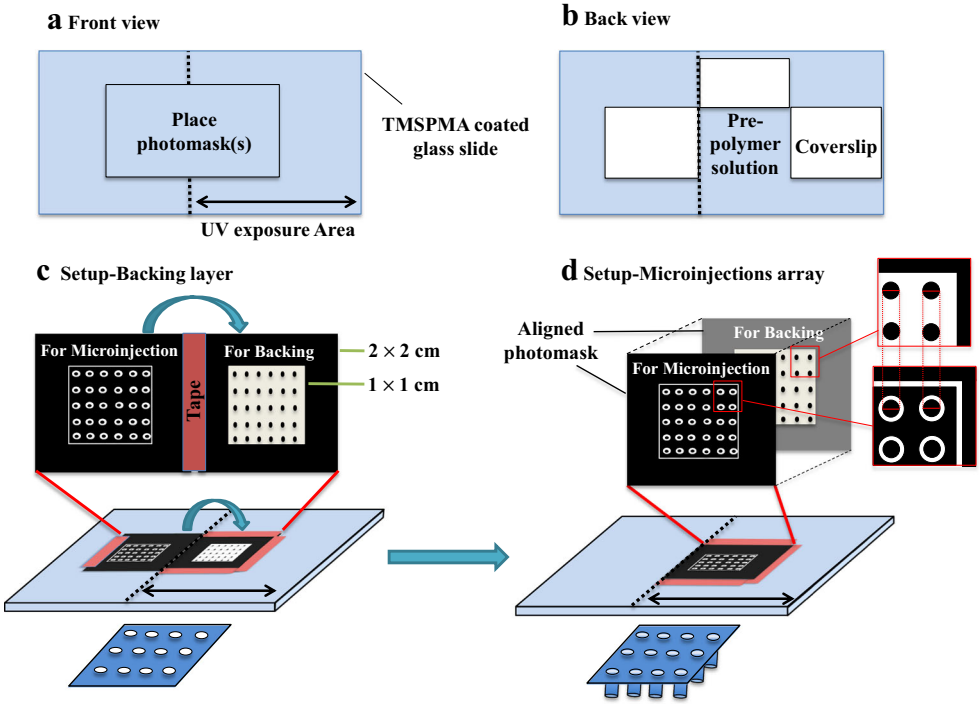

Fig. 1 Schematic of setup with UV exposure area defined. **a** Front view of setup. **b** Back view of setup. A cavity, measuring 1.5× 1.5 cm, was created using coverslips fitted down on either side. The height of the cavity is equivalent to the thickness of 1 coverslip. **c** Prealigning and assembling of photomasks on setup during fabrication of the backing layer. **d** Microinjection photomask folded over backing layer photomask for microinjection fabrication

for rigidization of the microinjections. The microinjections were imaged using Nikon SMZ25 stereomicroscope (Nikon, Japan). With the microinjections being colorless, it was difficult to view it under the stereomicroscope. Thus, for the purpose of imaging, 200 μL of rhodamine B 0.09 % *w/w* (Alfa Aesar, Lancaster, UK) solution was added into the prepolymer solution for the fabrication process.

Fabrication of plano-convex microlenses

Selection of polymer

Polymers' physical properties like viscosity, transparency, density, etc. may directly affect the fabrication of microlens. Three different molecular weight of PEGDA, i.e., PEGDA (Mn=250), PEGDA (Mn=575), and PEGDA (Mn=700),

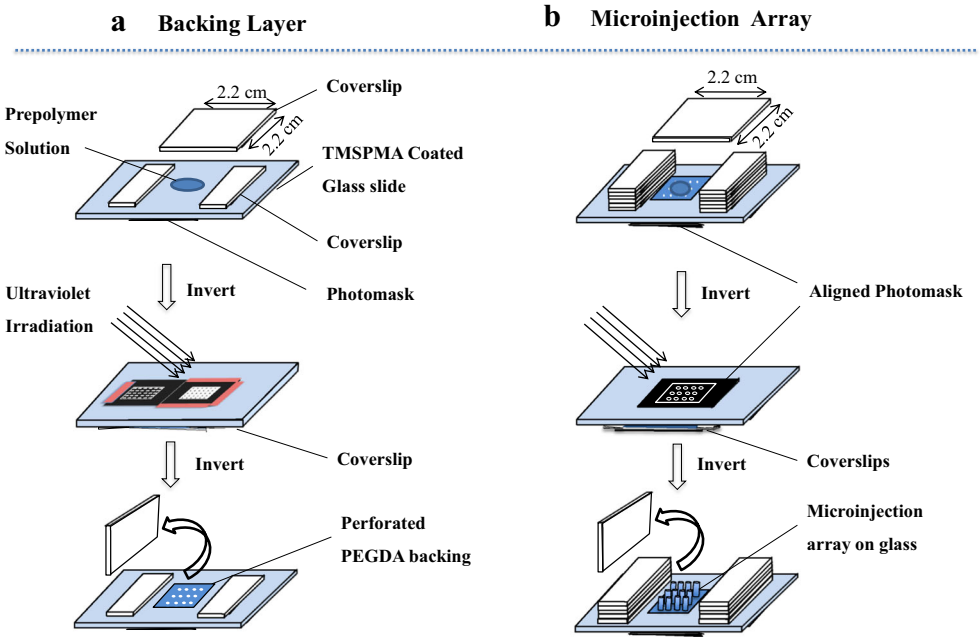

Fig. 2 **a** Schematic representation of the backing layer fabrication process. The setup was irradiated with UV through the backing layer photomask that was positioned prior to filling the cavity with prepolymer solution. **b** Schematic representation of the microinjection array fabrication process. The setup was irradiated again, this time through the microinjection photomask aligned over the backing layer photomask. Microinjections were created using cavity height of 5 coverslips thickness

were chosen for the preliminary assessment. All three polymers were similar in density, refractive index but different in the viscosity, where the PEGDA 700 had comparatively higher viscosity than the PEGDA 575 and PEGDA 250. These were further evaluated for selection based on dynamic contact angle measurements (see Dynamic contact angle).

Dynamic contact angle

PEGDA (Mn=250), PEGDA (Mn=575), and PEGDA (Mn=700) were individually mixed with 0.5 % *w/w* of HMP. From each solution, 1 μL using the pipette were placed onto glass coverslips to form droplets that were labeled according to time intervals 0, 5, 10, and 15 min. At the specified time points, the appropriately labeled coverslip with droplets from all three solutions was irradiated with high-intensity UV light (7.95 W/cm^2) for 3 s, at a distance of 10 cm from the UV source. The microlenses formed on each coverslip were imaged using Nikon SMZ25 stereomicroscope (Nikon, Japan). Dynamic contact angle and dimensions of each droplet were measured using the measurement tools (height, diameter, and free angle) from Nikon imaging software (NIS-Element Analysis D 4.20.00).

Fabrication of microlens array

A polydimethylsiloxane (PDMS) microinjection array stamp was used to fabricate plano-convex microlenses. A PDMS stamp (Fig. 5a) was first fabricated by curing a 10:1 mixture of silicone elastomer base solution and curing agent Sylgard 184 in a petri dish with a Combifix® Adapter (B. Braun Melsungen AG, Germany) placed in the center. The PDMS elastomer solution was degassed for 20 min in a vacuum chamber and cured at 70 °C for 2 h before the PDMS stamp was peeled from the petri dish [26]. A thin layer of elastomer solution was then applied onto the stamp, on the area surrounding the opening of the syringe adapter. The microinjection array was carefully placed over the opening of the adaptor, and the stamp was cured again at 70 °C for 1 h. This cemented the microinjection array onto the PDMS stamp with a complete seal around the opening of the syringe adapter. Only microinjections that were in direct contact with the opening of the syringe adaptor will have polymer solution flowing through them to form liquid microdroplets. Following the fabrication of the microinjection array stamp, 100 μL of PEGDA (Mn=700) containing 0.5 % *w/w* HMP was pipetted into the Combifix® Adapter (B. Braun Melsungen AG, Germany). The solution was allowed to pass through the microinjections and drain onto a piece of tissue. Another 100 μL of the solution was added at the same time, and after dabbing the stamp gently onto the tissue, the stamp was stamped onto an appropriate backing to produce liquid microdroplets. Before each stamping was carried out, the stamp has to be dabbed onto a piece of tissue to clean off any excess polymer solution surrounding the microinjections. Once the liquid microdroplets were produced, they were irradiated with high-intensity UV light (7.95 W/cm^2) for 5 s at a distance of 10 cm from the UV source (Fig. 5b), to form polymerized plano-convex microlenses.

Only 4 out of 49 microinjections in the 1×1 cm array were in direct contact with the opening of the syringe adapter, and thus, each produced a complete droplet of microlens capable of each microinjection. The four microlenses were then imaged using Nikon SMZ25 stereomicroscope (Nikon, Japan) prior to their fabrication into photomasks.

Fabrication of photomasks

The areas on the backing not covered by the microlenses were painted with Marabu 073 black glass paint (Marabu, Germany) using the Expression Series E81 size 15/0 detail spotter (Daler-Rowney, England). Five layers were applied with a 10-min drying interval between each layer (Fig. 5c).

Fabrication of microneedle shafts

Microneedles were fabricated using the photomask consisting of plano-convex microlenses that were fabricated previously. Firstly, to fabricate the microneedle shafts, a setup similar to Fig. 2b was used but having a coated coverslip placed over the cavity of desired spacer thickness. Also, backing layer and microinjection array photomasks were not used in this setup; instead, the photomask containing plano-convex microlenses was directly placed over the coated coverslip. The setup was irradiated with UV light at desired intensity and time of exposure, at a distance of 3.5 cm from the UV source. After polymerization, the photomask was removed for future use, and the coated coverslip now containing microneedles was removed from the setup, rinsed with water and dried with compressed air. Rigidization of the microneedles was carried out by exposing them to UV light (1.76 W/cm^2) for 3 s, at a distance of 3.5 cm from the UV source. The microneedles were imaged using Nikon SMZ25 stereomicroscope (Nikon, Japan). Since the microneedles were also colorless, for the purpose of imaging, 200 μL of rhodamine B 0.09 % *w/w* (Alfa Aesar, Lancaster, UK) solution was added into the prepolymer solution for the fabrication process.

Fabrication of microneedle backing

A backing layer had to be fabricated for the microneedle shafts prior to evaluating skin penetration efficiency. Two methods of creating the backing were being developed. First one, a thin layer of prepolymer solution was applied onto the TMSPMA-coated coverslip containing the microneedles. The coverslip was then irradiated with UV light (1.76 W/cm^2) for 4 s at a

distance 3.5 cm away from the UV source. The backing layer together with the microneedles were removed from the coverslip, rinsed with water, and dried with compressed air. In the second method, the backing layer was fabricated prior to the fabrication of the microneedle shafts. Initially, using a similar setup as shown in Fig. 1b, a cavity with a spacer thickness of 1-coverslip was created. A TMSPMA-coated coverslip was placed over the cavity prior to filling with prepolymer solution. The setup was irradiated with 1.76 W/cm^2 UV intensity for 2 s at a distance 3.5 cm away from the UV source. The coverslip with the backing layer was removed, rinsed with water, and then used to fabricate the microneedles shafts directly on it using steps as mentioned in Fabrication of microneedle shafts.

Microneedle penetration in cadaver human skin

Human dermatomed skin, donated by a 55-year-old, white male, was obtained from Science Care (Phoenix, AZ, USA). The use of human skin was approved by the National University of Singapore Institutional Review Board. The microneedles were assessed for skin penetration using three different methods. One, the microneedles were directly inserted into the skin. Two, the microneedles were treated with oxygen plasma for 1 min, flood-coated with trypan blue 0.4 % solution (Sigma-Aldrich, St. Louis, MO) and dried at 35 °C for 1 h.[27] Three, the microneedles were flood-coated with rhodamine B 0.1 % *w/w* (Alfa Aesar, Lancaster, UK) for 10 min and then rinsed with water. In all three methods, human skin obtained through posthumous organ donation was placed on a 6-mm-thick PDMS substrate mounted over a Styrofoam board with the epidermis side up.[28] A force of 10 N was applied through the applicator for 1 min, using force gauge (JSV H1000, JISC, Japan). The skin was then wiped with ethanol (70 %) and Kimwipes®. The application site was viewed using Nikon SMZ25 stereomicroscope (Nikon, Japan) using brightfield for methods 1 and 2 and using fluorescence in method 3.

Results

Fabrication of microinjection array

Fabrication of backing layer

Effect of varying UV intensity and time of exposure Triplicates of backing layers were formed for various times of exposure at 3.82, 5.90, and 7.95 W/cm^2 UV intensities. The various time of exposure points used were at every 0.5th second decrement from 3.5 to 0.5 s, with distance of exposure kept constant at 10 cm from the UV source. Backing layers formed were observed for its fragility and conductivity of liquids. Approximately 10 μL of PEDGA (Mn=700) was applied to each backing layer to test for its liquid conductivity, and if so, the solution will be absorbed onto a piece of tissue paper placed on the other side of the backing layer. Only the backing layer fabricated at UV intensity 3.82 W/cm^2 with a time of exposure of 1.5 s (Table 1) was able to show passing through of PEGDA (Mn=700) for all three triplicates.

Effect of varying dimensions of photomasks Backing layer photomasks of different inked circle dimensions of 200 μm and 300 μm were tested. The fragility and conductivity of PEGDA (Mn=700) through the backing layers produced from both photomasks were comparable and were observed to have similar results as that mentioned above. For both, a UV intensity of 3.82 W/cm^2 with a time of exposure of 1.5 s was the only set of triplicates that had a balance between fragility and liquid conductivity.

Fabrication of microinjections

Effect of varying time of exposure Microinjections without the backing layer were first made to determine which time of exposure would be appropriate. A UV intensity of 7.95 W/cm^2 was used with a distance of 10 cm from the UV source. Different exposure times of 2, 2.5, and 3 s were used, and it was observed that at 2 and 2.5 s, microinjections fabricated were cylindrically shaped and visibly hollow as desired. At 3 s, a layer of polymer blocking the tips of the microinjections was observed. This phenomenon was not observed in the 2.5 and 2 s exposure times.

Effect of varying dimensions of photomasks Varying designs of backing layer photomasks were used together with different microinjection photomasks to form microinjection arrays (Table 2). The backing layer photomasks only contain inked circles while microinjection photomasks consist of inked circles of similar diameters to the

Table 1 Comparison of UV intensities at 3.82, 5.90, or 7.95 W/cm^2 at different time exposures

	UV intensity (W/cm^2)		
Time (s)	7.95	5.90	3.82
3.5	×	×	×
3	×	×	×
2.5	×	×	×
2	×	×	×
1.5	×	×	✓
1	×	×	Brittle
0.5	Brittle	–	–

× PEGDA700 was unable to pass through, –backing layer was not formed completely, ✓ PEGDA700 were able to pass through the triplicates

Table 2 Summary of circle dimensions patterned on different pairs (A, B, or C) of backing layer and microinjection photomasks

Diameter (μm)			
Pair	Inked circle	Outer circle	Thickness
A	200	600	200
B	300	400	50
C	300	500	100

Backing layer photomasks only contain inked circles while microinjection photomasks consist of inked circles of similar diameters to the backing layer photomask it is paired with and surrounding outer circles of larger dimensions. Each outer circle surrounds the inked circle such that there is a clear transparent ring of a certain thickness, which will be equivalent to the thickness of the resultant microinjection walls. Pair C was the chosen pair of photomasks used

backing layer photomask it was paired with and surrounding outer circles of larger dimensions. Each outer circle surrounds the inked circle in the microinjection photomask such that there was a transparent ring of a certain thickness, as seen in Fig. 1c. When both photomasks were overlapped to form microinjection array, this thickness was equivalent to the thickness of the resultant microinjection walls. Microinjections fabricated from pair A were observed to have blockage. The base of the microinjections also had reduced inner diameters of approximately 80 μm. Subsequently, pair B was used, and the microinjections were observed to be incompletely formed. Manual alignment of both photomasks was also difficult due to the small dimensions of the circles. In consideration of both pairs of photomasks initially experimented on, another pair of photomasks was used, pair C. The microinjections formed were observed to be hollow throughout with an inner base diameter approximating 200 μm, an outer tip diameter approximating 500 μm, and an inner tip diameter approximating 400 μm (Fig. 3). This suggested that the thickness of the transparent ring on the photomasks could indeed fabricate microinjection walls of equivalent thickness. Alignment in pair C was also easier which led to less instances of misalignment. Misalignment of the photomasks could lead to incompletely formed microinjections or microinjections with thickened walls, leading to reduced inner diameters. This could affect the volume of liquid expelled from each microinjection to form the microlenses.

Following the fabrication of the microinjections, all microinjections of an array were proved to be fully functional by simply pipetting PEGDA solution onto the backing layer of the microinjection array and determine if the solution was able to pass through the microinjection tips and be absorbed onto a piece of Kimwipes. Also, the microinjections were also seen to be hollow using the stereomicroscope.

Fabrication of microlenses

Dynamic contact angle

Characterization of droplets formed from PEGDA of varying molecular weights which also varied in viscosity was done to determine the effect on the droplet size over a period of different intervals. The higher the molecular weight PEGDA used, the larger the contact angle of the droplet was observed as shown in Fig. 4. PEGDA (Mn=250) microlens was observed to be comparably flat at time 0 min, while PEGDA (Mn=700) microlens was observed to retain its shape even after 10 min.

Stamping

Triplicates of microlens array were produced from the fabricated microinjection array stamp. A stereomicroscopic image of the microlenses has been shown in Fig. 5e. The average height and diameter of the four microlenses from each coverslip were measured. The pooled average height of 12 microlenses was 135.5±24.4 μm while the pooled average diameter was 734.5±90.0 μm. The radius of curvature of the microlenses was calculated using the following equation with the pooled averages:

$$R = \frac{(K+1)h^2 + (\varnothing \div 2)^2}{2h} \tag{1}$$

where R is the radius of curvature, $\varnothing$ is the diameter of the microlens, K is the aspheric constant, and h is the height. The aspheric constant (K) of a spherical plano-convex lens is 0 [29]. The radius of curvature calculated using the pooled averages was 565.4 μm.

The contact angle (α) of a plano-convex lens is also given by

$$\sin\alpha = r \Big/ R \tag{2}$$

where r is the radius of the microlens. For the microlenses fabricated, the contact angle was 40.6±6.0.

Fabrication of photomask

Water-based glass paint was colored onto areas using the spotter and carefully controlled not to spread over the microlenses (Fig. 5f). Physical properties of the microlenses remained approximately the same after painting. As for optical properties, the focal length (f) produced from these microlenses were estimated to be 1203.0 μm via the lens maker's equation as stated below:

$$\frac{1}{f} = \left(\frac{n_l}{n_m} - 1\right) \times \left(\frac{1}{r_1} - \frac{1}{r_2}\right) \tag{3}$$

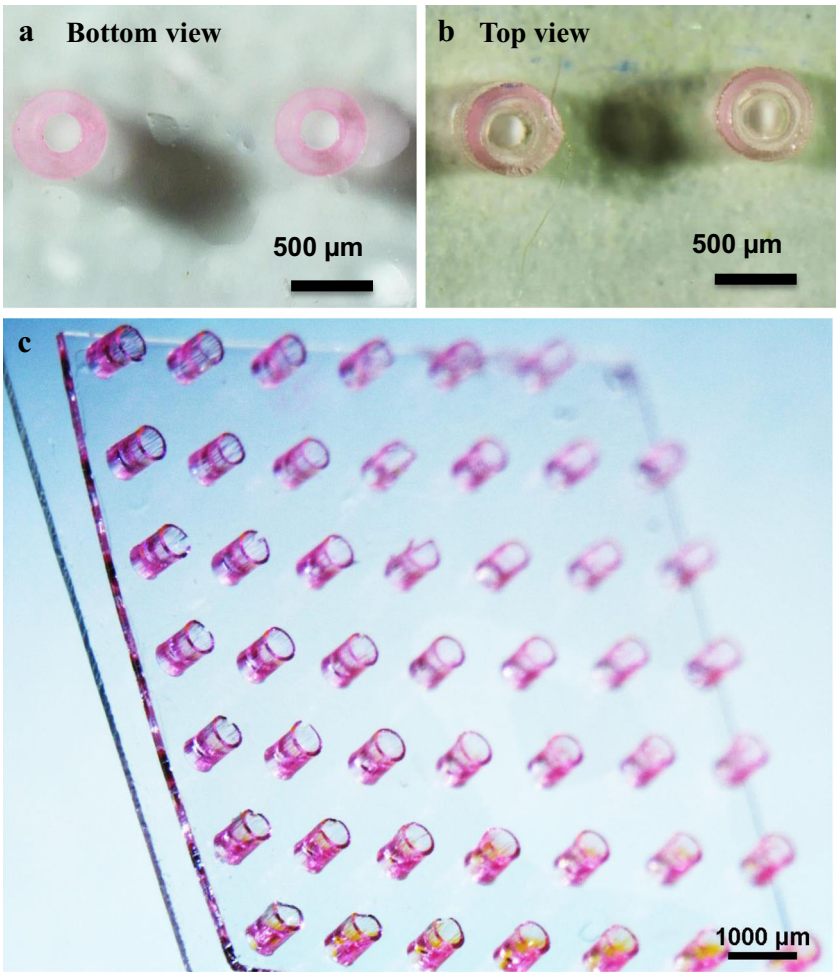

Fig. 3 **a** Back view of the base of two microinjections. **b** Top view of two microinjection tips. **c** Image of microinjection array

where n_1 is the refractive index of the lens material PEGDA (Mn=700) (1.47), n_m is the refractive index of ambient medium, air (1.00) at a wavelength of 365 nm, r_1 is the radius of curvature of the first surface, r_2 is the radius of curvature of the second surface, which is ∞ ($1/r_2=0$) for a plano-convex lens. The photomask was then tested for its use in microneedle fabrication.

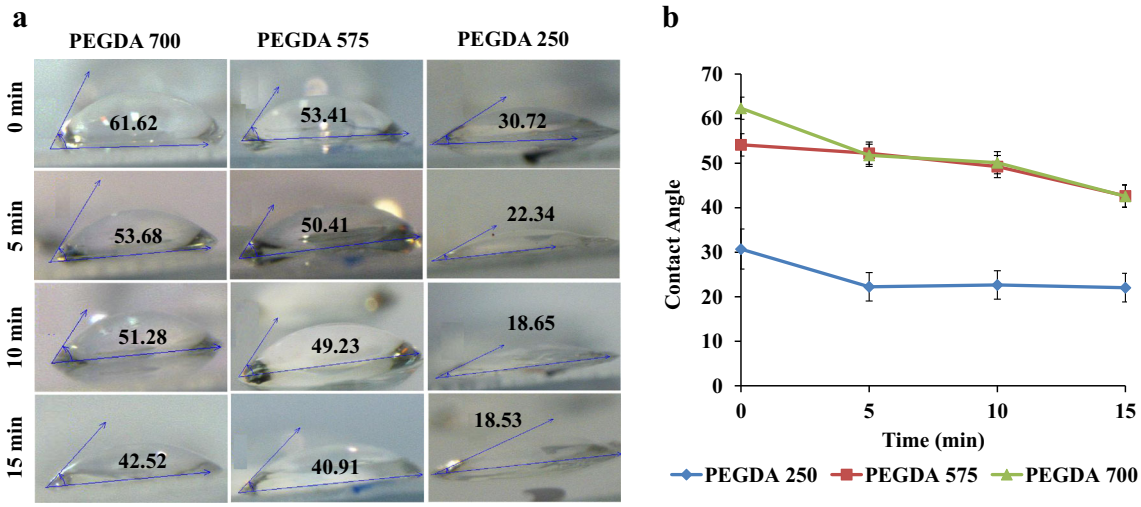

Fig. 4 Contact angle of PEGDAs at 1 μL each on the glass coverslip. **a** Images of polymerized droplets with contact angle. **b** Contact angle of PEGDAs of varied molecular weight with respect to time

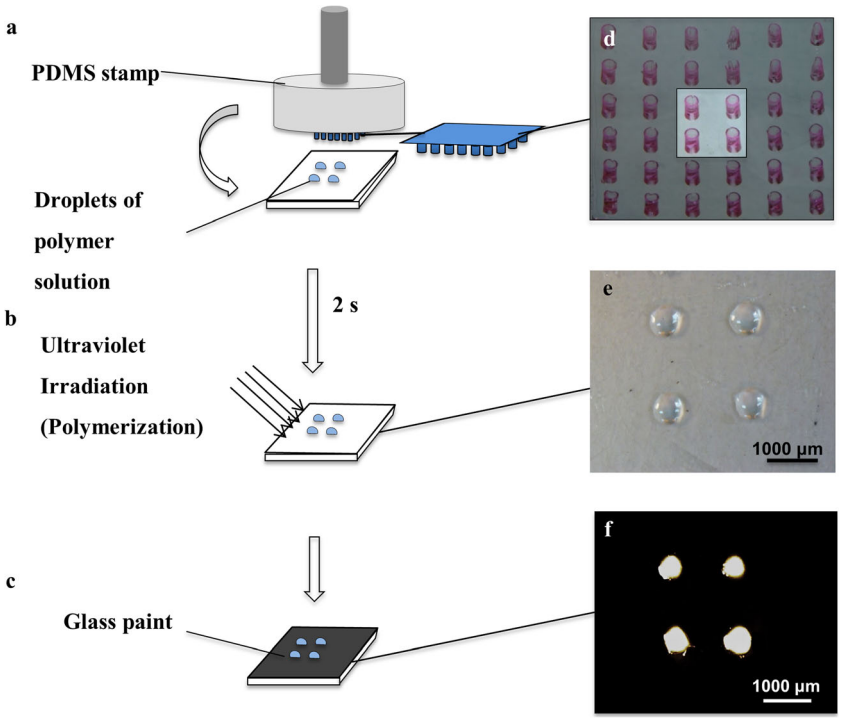

Fig. 5 Schematic of photomask consisting microlense fabrication process. **a** Fabricated microinjection array integrated onto the PDMS stamp was applied onto the glass coverslip to create droplets of polymer solution. **b** The liquid droplets were immediately irradiated with UV to form solidified plano-convex microlenses. **c** Application of paint onto the glass to create photomask. **d** Image of microinjection array, showing the bright and fade region. Only bright region was allowed to be functional for stamping. **e** Image of plano-convex microlenses. **f** Image of photomask consisting microlenses

Fabrication of microneedle shafts

Photomask consisting plano-convex microlenses enabled the UV light to focus at a focal point to form tapered microneedles. In combination with the use of the photomask containing plano-convex microlenses, microneedle fabrication was also further enhanced with the optimization of other parameters such as UV intensity, spacer thickness, and time of exposure.

Firstly, microneedles were fabricated at varying UV intensities with a constant spacer thickness 900 μm, and a time of exposure of 1 s, at a distance 3.5 cm away from the UV source. It was observed that as UV intensity decreased, tip diameter and length of the microneedles also decreased, with 1.76 W/cm^2 UV intensity producing the sharpest and shortest microneedles (Fig. 6a, b). Next, the microneedles were fabricated using varying spacer thickness at a constant UV intensity of 1.76 W/cm^2, a time of exposure of 1 s, and a distance 3.5 cm away from the UV source. As expected, it was observed that as spacer thickness increased, the tip diameter decreased with increasing length of the microneedles, especially at 4000 μm (Fig. 6c, d). Lastly, the time of exposure was varied to observe its effect on microneedle fabrication. A constant UV intensity (1.76 W/cm^2), spacer thickness (4000 μm), and distance of exposure (3.5 cm) was used. It was observed that as time of exposure increased, the length of the microneedles increased without significant change in the tip diameters (Fig. 6e).

Therefore, with optimized parameters of 1.76 W/cm^2 for UV intensity, time of exposure of 1 s, and a distance of exposure of 3.5 cm, sharp polymeric microneedles 1650± 132 μm in length, a tip diameter of 33.1±5.7 μm, and an aspect ratio of approximating 5:1 were fabricated (Fig. 7a, b).

Fabrication of microneedle backing

Two methods of fabricating backing layer for microneedle shafts were being investigated. Both methods were able to fabricate microneedles that had sufficient rigidity. Even though both methods were vastly different, both did not produce microneedles of significant difference in terms of its length or tip diameters. Thus, any of the two methods would be suitable for use in this fabrication process.

Microneedle penetration in cadaver human skin

Insertion of microneedles through cadaver human skin could be observed in all three methods: firstly, through the insertion marks as in seen in Fig. 7c. Secondly, penetration was also observed via trypan blue-stained punctured dots that remained on the skin (data not shown). In the third method, fluorescence of rhodamine B could be observed by four distinct dots that were created following its penetration (Fig. 7d).

Discussion

In this study, a method of using a microinjection array for the purpose of fabricating photomasks consisting plano-convex

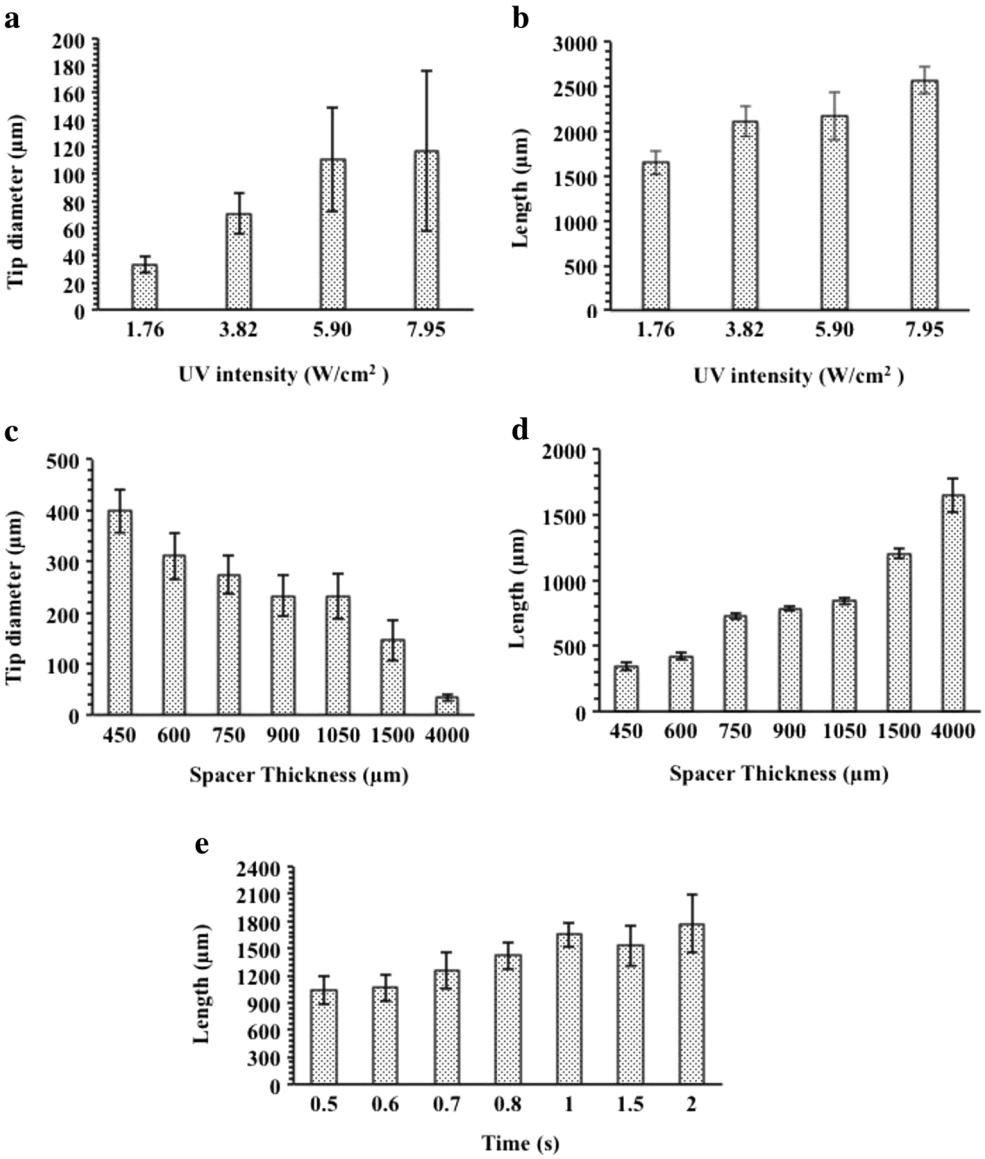

Fig. 6 **a** Tip diameters of microneedles when UV intensity was varied. **b** Length of the microneedles when UV intensity was varied. **c** Using a constant UV intensity of 1.76 W/cm^2, tip diameters of microneedles varied with different spacer thickness. **d** Using a constant UV intensity of 1.76 W/cm^2, length of microneedles varied with different spacer thickness. **e** Using a constant UV intensity of 1.76 W/cm^2 and spacer thickness of 4000 μm, microneedle length did not vary much with different times of exposure

microlenses has been presented. Microinjection array was first fabricated using a two-step photolithographic approach and then incorporated into a stamp to produce liquid microdroplets. These liquid microdroplets were polymerized and made into a photomask, which was used to converge the UV light path to fabricate sharp polymeric needles. Therefore, in order to produce microlenses of desired geometric profiles, the physical properties of the microinjection array such as the height, diameter, and rigidity had to be optimized.

Fabrication of microinjection array

The backing layer and microinjection tips were two essential components to the microinjection array. The backing layer had to possess microwell-like structures in order to act as a hollow base for the microinjections. When the backing layer was initially fabricated without the microinjections, varying the dimensions of the backing layer photomask did not significantly affect the ability of PEGDA (Mn=700) to pass through. However, when the microinjection tips were fabricated onto the backing layer, the microwell structures in the backing layer greatly reduced in diameter. This could be due to increased polymerization of the backing layer during microinjection fabrication where it was exposed to another round of UV light. When microinjection array was fabricated using pair A, the microinjections were observed to be closed off due to the great thickness of the walls. This suggested that a reduction in wall thickness was necessary and therefore implied that the microinjection photomask used should possess transparent rings of reduced thickness. However, when wall thickness was reduced to approximately 50 μm, as in pair B, the microinjections were incompletely formed and were fragile. Thus, a balance between

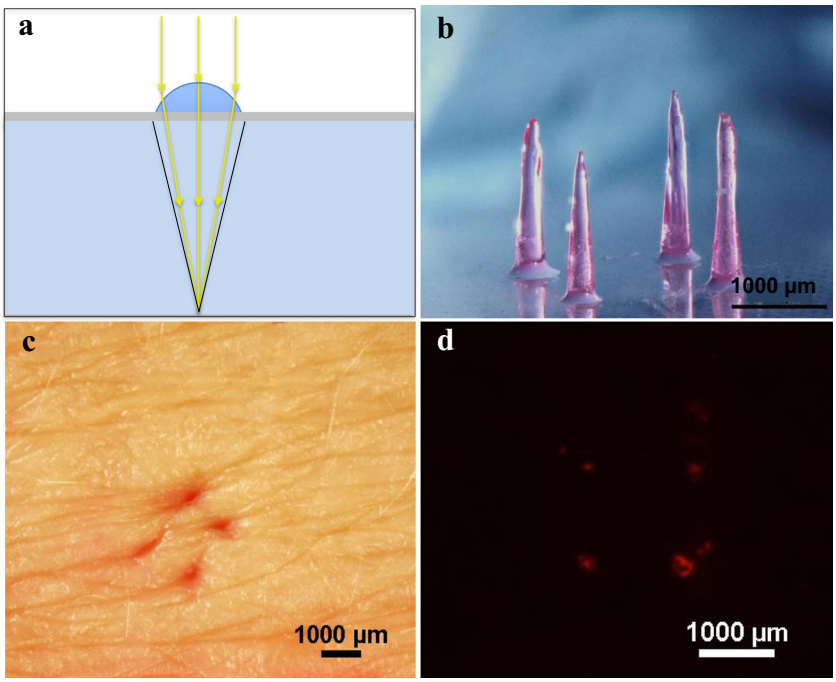

Fig. 7 **a** UV light refracts on the surface of the lens to focus UV light into a conical light path, producing tapered microneedles. **b** Side view of the microneedles (*inverted*). **c** Image of skin following microneedle insertion. **d** Skin penetration assessed using fluorescence following skin penetration of rhodamine B

preserving the microwell structures of the backing layer and the fragility of the microinjections had to be optimized. Therefore, a 300-μm backing layer photomask and a microinjection photomask having transparent rings of 100 μm thickness, as in pair C, was used in the final fabrication method of the microinjections as it was the only pair which presented with such a balance (Table 2).

The microinjections fabricated from pair C were cylindrical in shape and were hollow. However, when inner diameters of different parts of the microinjection were measured, it gradually increased from the base to the tip of the microinjection. This could be due to the change in diffraction of UV light as it passes through the photomask and as the microinjection forms. This could have increased the volume of polymer solution individual microinjections could hold.

Using two methods, i.e., PEGDA pass through and stereomicroscopy, it was confirmed that all the microinjections within the array were fully functional and any of the microinjections can be used further. Therefore, in order to prove the concept of fabrication of the microlens using this method, only 4 out of the 49 microinjections within the array were used. For upscaling the fabrication of microlens array, the assembly of the PDMS microinjection stamp (see Dynamic contact angle and Fig. 5) can be modified to allow PEGDA to pass through more number of microinjections (>2×2 array). This allows the formation of bigger array of microdroplet and hence the bigger array of microlens after photolithography. The author recommends the use of controlled system or machinery to control the passage of PEGDA to form the microdroplets for further improvements and upscaling of microlens array.

Fabrication of microlenses

The fabrication of microlenses starts off with the selection of polymer and backing, as both were essential in the resultant characterization of the plano-convex microlenses. Firstly, the choice of the polymer solution used was greatly influenced by its molecular weight and viscosity. The higher the molecular weight of PEGDA used, the greater the viscosity [30], and thus, droplets of more desirable geometric profiles were produced. Furthermore, as shown in Fig. 4, PEGDA 700 was found to have higher contact angle on glass coverslip than other low molecular weight PEGDA. Contact angle were found to be dependent on time for all three types of PEGDA. However, the decrease in the contact angle for PEGDA 700 and PEGDA 575 was still much higher than PEGDA 250 after 15 min. Therefore, PEGDA 700 as the polymer solution on glass coverslips was amenable for the fabrication of plano-convex microlenses. The change in contact angle can be attributed to the inertial and viscous effects of contact angle which might be a cause of dynamic interfacial interaction of liquid droplets with solid glass surface and its dependency on time [32–34].

To construct a photomask that was able to fabricate sharp polymeric needles, the geometry of the microlenses had to be optimized. Characteristics of the microlenses determine the degree of refraction of UV light rays on the convex surface.

Thus, the height, diameter, contact angle, and radius of curvature of the microlenses were measured following fabrication. Microlenses produced from the microinjection array via stamping had a relatively large diameter and a small height. Their geometric profiles also varied slightly from one another whether it was within the same set of triplicates belonging to one microinjection array or between other sets of triplicates when another microinjection array was used. This could be due to the manual approach of the stamping method, where pressure or angle applied from stamp onto the coverslip may vary each time.

Fabrication of photomask and microneedles

Photomask containing microlenses was fabricated by application of several layers of glass paint onto the surrounding areas of the microlenses. The darkened areas of the photomask were able to block the access of UV light to the polymer solution, which prevented any unnecessary polymerization. The spotter brush was also able to avoid accidental application of paint onto the microlenses, allowing the microlenses to remain transparent.

Since the microlenses were the only areas of the photomask that remained optically transparent, UV light was able to refract on the surface of the lens, converge at a focal point to form sharp polymeric microneedles. Microneedle geometry was not only influenced by the geometric profile and optical properties of the microlenses on the photomask; UV parameters such as intensity, time of exposure, distance of exposure, and spacer thickness play an essential role. Therefore, UV intensity and spacer thickness used in this study also had to be optimized for the fabrication of microneedles, while time and distance of exposure were kept constant, following a previous study [23]. Firstly, when all other variables were kept constant, it was observed that an UV intensity of 1.76 W/cm^2 produced the least deformed, smallest tip diameter and highest vertical length microneedles as compared to higher UV intensities (3.82, 5.90, and 7.95 W/cm^2). Thus, it was chosen as the UV intensity for this study. Secondly, in order to optimize spacer thickness, varying thickness of coverslips ranging from 450 to 1500 μm were used to fabricate microneedles. It was observed that as spacer thickness increased, height of the microneedles increased and tip diameters decreased. However, even at a spacer thickness of 1500 μm, the microneedles were blunt and had a conical shape rather than a sharp tip. Therefore, in order to prevent spacer thickness from being a limiting factor for polymerization to occur maximally, spacer thickness was increased to approximately 4000 μm. This thickness allowed the microneedles to polymerize without hindrance, to its maximal vertical length, resulting in the production of short tapered microneedles with small tip diameters. The true focal length of the microlenses on the photomask was also reflected at this spacer thickness.

In several studies involving fabrication of the microlens arrays, the focal length of the microlenses produced was estimated via the lens maker's equation. In Fig. 7a, the focal point at which light converges is equivalent to the tip of the microneedles, while the focal length is equivalent to the length of the microneedles. In the previous study done in our lab, the focal length calculated was three times less than the actual length of the microneedles fabricated regardless of UV intensity used. This could be due to the flat top surface of the microlens in the photomask, which could have led to spherical aberration of light. Therefore, it was suggested that the equation was not a good predictive model for the fabrication process [23]. Conversely, in this study, the focal length calculated based on the equation was able to approximate the length of the microneedles fabricated when a spacer thickness of 4000 μm was used. This suggests that the lens maker's equation may potentially be an accurate predictive model in this fabrication process. However, this equation still may not be the best reflection of the true focal length of microneedles fabricated using photolithographical approach, even when a photomask consisting plano-convex microlenses is used. As photopolymerization is a continuous and dynamic process, which continuously takes place during fabrication of the microneedles, the refraction of UV light is also continuously being varied. This can be attributed to a matrix effect, in which PEGDA in the liquid state, during or after polymerization, may not refract UV light in same manner. Furthermore, the equation does not take into account the UV parameters such as intensity, distance, and time of exposure, which also greatly influences microneedle fabrication. Hence, the lens maker's equation may not be suitable predictive model for the microneedles fabricated using photopolymerization.

Microneedle penetration in cadaver human skin

Insertion of the microneedls into skin could be observed in all three methods of assessing microneedle skin penetration. Firstly, microneedle insertion could be observed by the insertion marks in the skin and also via the blue dots created by trypan blue when the coated microneedles pierced through the skin. Trypan blue, being hydrophobic in nature, stained the perforated hydrophobic SC. Secondly, rhodamine B was seen to fluorescence at only four distinct dots on the skin. Rhodamine B stains skin easily regardless of microneedle penetration. Here, microneedles and its backing layer were being flood-coated with rhodamine B, and thus, the whole patch was stained. During application of the microneedles, the backing layer was also in contact with the skin, which would leave traces of rhodamine B on the surrounding skin even after wiping. However, only marks made by the four microneedles showed fluorescence, which supports the penetration of microneedles. This could be due to rhodamine B being soluble in water associated with the dermal layer of skin when the

microneedles penetrated, leading to fluorescence only in penetrated region on skin.

Further optimization of this microlense fabrication method using microinjection arrays is still required to produce a bigger array of microlenses. This would, in turn, also lead to photomasks consisting of more microlenses that are able to fabricate larger microneedle arrays. Nevertheless, through the successful fabrication of short tapered microneedles in this study, apart from the UV parameters being optimized, it suggests that the photomask consisting plano-convex microlenses fabricated using this method can perform its function efficiently.

Conclusion

In this study, the microinjection array was shown to be capable of producing plano-convex microlenses that possessed appropriate geometric properties. Photomask consisting microlens array was successfully fabricated using a microinjection array. Photomask fabrication was simple and was able to produce polymeric microneedles, which were shorter and sharper. It can also potentially enhance skin penetration efficiency as demonstrated in cadaver human skin. This approach can be of potential use to fabricate sharp microneedle arrays of various dimensions using the photomask consisting microlenses by varying the dimensions of microlens. It can also be of potential use to fabricate the hollow polymeric microneedle array.

Acknowledgments The authors thank Dr. Jaspreet Singh Kochhar from P&G Singapore, Dr. Pan Jing, and Ms. Li Hairui from the National University of Singapore for their helpful discussions.

Conflict of interest The authors declare no conflict of interest.

References

1. Daugimont L, Baron N, Vandermeulen G, Pavselj N, Miklavcic D, Jullien MC, et al. Hollow microneedle arrays for intradermal drug delivery and DNA electroporation. J Membr Biol. 2010;236(1):117–25.
2. Paudel KS, Milewski M, Swadley CL, Brogden NK, Ghosh P, Stinchcomb AL. Challenges and opportunities in dermal/transdermal delivery. Ther Deliv. 2010;1(1):109–31.
3. Lhernould MS. Optimizing hollow microneedles arrays aimed at transdermal drug delivery. Microsyst Technol. 2013;19(1):1–8.
4. Kaestli LZ, Wasilewski-Rasca AF, Bonnabry P, Vogt-Ferrier N. Use of transdermal drug formulations in the elderly. Drugs Aging. 2008;25(4):269–80.
5. Kenneth A. Walters MSR. Dermatologic, cosmeceutic and cosmetic development. 1st ed. Informa Healthcare; 2007.
6. Escobar-Chávez JJ, Bonilla-Martínez D, Angélica M, Villegas G, Molina-Trinidad E, Casas-Alancaster N, et al. Microneedles: a valuable physical enhancer to increase transdermal drug delivery. J Clin Pharmacol. 2011;51(7):964–77.
7. Kim YC, Park JH, Prausnitz MR. Microneedles for drug and vaccine delivery. Adv Drug Deliv Rev. 2012;64(14):1547–68.
8. Indermun S, Luttge R, Choonara YE, Kumar P, du Toit LC, Modi G, et al. Current advances in the fabrication of microneedles for transdermal delivery. J Control Release. 2014;185(0):130–8.
9. Bariya SH, Gohel MC, Mehta TA, Sharma OP. Microneedles: an emerging transdermal drug delivery system. J Pharm Pharmacol. 2012;64(1):11–29.
10. Park JH, Allen MG, Prausnitz MR. Biodegradable polymer microneedles: fabrication, mechanics and transdermal drug delivery. J Control Release. 2005;104(1):51–66.
11. Wilke N, Mulcahy A, Ye SR, Morrissey A. Process optimization and characterization of silicon microneedles fabricated by wet etch technology. Microelectron J. 2005;36(7):650–6.
12. Schlingloff G, Kiel HJ, Schober A. Microlenses as amplification for CCD-based detection devices for screening applications in biology, biochemistry, and chemistry. Appl Opt. 1998;37(10):1930–4.
13. Roulet JC, Volkel R, Herzig HP, Verpoorte E, de Rooij NF, Dandliker R. Fabrication of multilayer systems combining microfluidic and microoptical elements for fluorescence detection. J Microelectromech Syst. 2001;10(4):482–91.
14. Stevens R, Harvey T. Lens arrays for a three-dimensional imaging system. J Opt A Pure Appl Opt. 2002;4(4):S17.
15. He M, Yuan XC, Ngo NQ, Bu J, Tao SH. Single-step fabrication of a microlens array in sol–gel material by direct laser writing and its application in optical coupling. J Opt A Pure Appl Opt. 2004;6(1):94.
16. Sunghyun Y, Joon-Geun H, Joo-Young J, Chang-Hyeon J, Yong-Kweon K. Monolithically integrated glass microlens scanner using a thermal reflow process. J Micromech Microeng. 2013;23(6):065012.
17. Lian ZJ, Hung SY, Shen MH, Yang H. Rapid fabrication of semiellipsoid microlens using thermal reflow with two different photoresists. Microelectron Eng. 2014;115(0):46–50.
18. He M, Yuan XC, Ngo N, Bu J, Kudryashov V. Simple reflow technique for fabrication of a microlens array in solgel glass. Opt Lett. 2003;28(9):731–3.
19. Xiangwei M, Feng C, Qing Y, Hao B, Hewei L, Pubo Q, et al. A simple way to fabricate close-packed high numerical aperture microlens arrays. IEEE Photon Technol Lett. 2013;25(14):1336–9.
20. Kuo JN, Hsieh CC, Yang SY, Lee GB. An SU-8 microlens array fabricated by soft replica molding for cell counting applications. J Micromech Microeng. 2007;17(4):693.
21. Kuo SM, Lin CH. Fabrication of aspherical SU-8 microlens array utilizing novel stamping process and electro-static pulling method. Opt Express. 2010;18(18):19114–9.
22. Park JH, Yoon YK, Choi SO, Prausnitz MR, Allen MG. Tapered conical polymer microneedles fabricated using an integrated lens technique for transdermal drug delivery. IEEE Trans Biomed Eng. 2007;54(5):903–13.
23. Kochhar J, Anbalagan P, Shelar S, Neo J, Iliescu C, Kang L. Direct microneedle array fabrication off a photomask to deliver collagen through skin. Pharm Res. 2014;31(7):1724–34.
24. de Groot JH, van Beijma FJ, Haitjema HJ, Dillingham KA, Hodd KA, Koopmans SA, et al. Injectable intraocular lens materials based upon hydrogels. Biomacromolecules. 2001;2(3):628–34.
25. Kochhar JS, Goh WJ, Chan SY, Kang L. A simple method of microneedle array fabrication for transdermal drug delivery. Drug Dev Ind Pharm. 2013;39(2):299–309.
26. Pan J, Yung Chan S, Common JE, Amini S, Miserez A, Birgitte Lane E, et al. Fabrication of a 3D hair follicle-like hydrogel by soft lithography. J Biomed Mater Res A. 2013;101(11):3159–69.
27. Li H, Low Y, Chong H, Zin M, Lee CY, Li B et al. Microneedle-mediated delivery of copper peptide through skin. Pharm Res. 2015;32(8):2678–89.

28. Kochhar JS, Quek TC, Soon WJ, Choi J, Zou S, Kang L. Effect of microneedle geometry and supporting substrate on microneedle array penetration into skin. J Pharm Sci. 2013;102(11):4100–8.
29. Nussbaum P, Voelkel R, Herzig HP, Eisner M, Haselbeck S. Design, fabrication and testing of microlens arrays for sensors and microsystems. Pure Appl Opt: J Eur Opt Soc Part A. 1997;6(6):617.
30. Moon BU, Tsai SH, Hwang D. Rotary polymer micromachines: in situ fabrication of microgear components in microchannels. Microfluid Nanofluid. 2015;19(1):1–8.
31. Cox RG. Inertial and viscous effects on dynamic contact angles. J Fluid Mech. 1998;357(1):249–78.
32. Welygan DG, Burns CM. Dynamic contact angles of viscous liquids. J Adhes. 1980;11(1):41–55.
33. Tan G, Wang Y, Li J, Zhang S. Synthesis and characterization of injectable photocrosslinking poly (ethylene glycol) diacrylate based hydrogels. Polym Bull. 2008;61(1):91–8.
34. Rupp F, Axmann D, Ziegler C, Geis-Gerstorfer J. Adsorption/desorption phenomena on pure and teflon AF-coated titania surfaces studied by dynamic contact angle analysis. J Biomed Mater Res. 2002;62(4):567–78.